IN-24
21277

NASA Technical Memorandum 105166

Interphase Layer Optimization for Metal Matrix Composites With Fabrication Considerations

M. Morel
Sverdrup Technology, Inc.
Lewis Research Center Group
Brook Park, Ohio

D.A. Saravanos
Case Western Reserve University
Cleveland, Ohio

and

C.C. Chamis
National Aeronautics and Space Administration
Lewis Research Center
Cleveland, Ohio

Prepared for the
36th International SAMPE Symposium and Exhibition
San Diego, California, April 15-18, 1991

NASA

INTERPHASE LAYER OPTIMIZATION FOR METAL MATRIX COMPOSITES WITH FABRICATION CONSIDERATIONS

M. Morel *

Sverdrup Technology, Inc.

Lewis Research Center Group

Brookpark, Ohio 44142

D. A. Saravanos **

Case Western Reserve University

Cleveland, Ohio 44106

C. C. Chamis ***

National Aeronautics and Space Administration

Lewis Research Center

Cleveland, Ohio 44135

ABSTRACT

A methodology is presented to reduce the final matrix microstresses for metal matrix composites by concurrently optimizing the interphase characteristics and fabrication process. Application cases include interphase tailoring with and without fabrication considerations for two material systems, graphite/copper and silicon carbide/titanium. Results indicate that concurrent interphase/fabrication optimization produces significant reductions in the matrix residual stresses and strong coupling between interphase and fabrication tailoring. The interphase coefficient of thermal expansion and the fabrication consolidation pressure are the most important design parameters and must be concurrently optimized to further reduce the microstresses to more desireable magnitudes.

---

* *Research Engineer.*

** *Research Associate.*

*** *Senior Aerospace Scientist.*

NOMENCLATURE

d_f	Fiber diameter.
E	Young's Modulus.
$F(z)$	Objective function.
G	Shear Modulus.
h_i	Interphase thickness.
k	Volume ratio.
P	Property.
p	Pressure.
$Q(z)$	Inequality constraint.
S	Ultimate Strength.
T	Temperature.
T_M	Melting temperature.
t	Time.
w	Weight coefficient.
z	Optimization Parameter.
α	Thermal expansion coefficient.
ρ	Mass Density.
σ	Stress or Microstress.
ν	Poisson's ratio.

Superscripts

L	Lower bound.
t	Time.
U	Upper bound.

Subscripts

C	Compression.
f	Fiber.
i	Interphase.
m	Matrix.

l	Unidirectional composite.
n	Normal.
o	Reference.
s	Shear.
T	Tension.
$1, 2, 3$	Composite material coordinate system axes.

1. INTRODUCTION

Applications of metal matrix composites (MMCs) in the aerospace industry are becoming a more viable solution for property demands in terms of high temperature resistance, high modulus, strength, hardness, conductivity, dimensional stability, and low density. Yet, two significant issues counteracting the merits of MMCs are the large residual stresses and the apparently weak interface between the fibers and matrix. Due to the mismatch of the coefficient of thermal expansion (CTE) between the fiber and matrix, relatively large residual stresses develop in the composite during its fabrication. These high stresses degrade the mechanical properties, either by reducing the in situ properties of the matrix or by initiating matrix microcracking, and lower the thermo-mechanical fatigue (TMF) life of the composite [1-3].

The residual stresses are strongly affected by a number of parameters: (1) the fiber/matrix properties, such as, CTE mismatch, moduli, and yield strengths; (2) the interphase CTE, modulus, and strength; (3) interphase thickness and fiber volume ratio; and (4) the processing temperature and pressure histories. Hence, the residual stresses may be controlled by either altering the fabrication parameters or by adding a compatible interphase layer between the fiber and matrix. Recent work on the reduction of the residual stresses in MMCs involved optimization of the fabrication process in terms of temperature and consolidation pressure histories [4], interphase tailoring based on an elastic three-cylinder model neglecting temperature effects [5], and parametric studies based on a slightly more complicated three-cylinder model that included plasticity [6]. But a combined interphase layer and fabrication process optimization can provide wider margins for controlling residual stresses in MMCs, thereby, improving mechanical performance and

TMF endurance.

The objective of this paper, therefore, is to define a methodology to optimize the interphase properties concurrently with the fabrication parameters necessary to: control residual microstresses during fabrication; prevent failures in the fiber, interphase, and matrix; and evade reductions in the mechanical properties of the fabricated composite. The development of this computational procedure is discussed herein; whereas nonlinear composite mechanics are used to simulate the characteristic behavior of the composite system during fabrication. The composite mechanics include inelastic and temperature effects on the matrix and interphase which provide more accurate predictions of residual stresses and entail the capacity to capture the coupling between the fabrication and interphase properties. For the optimization, the feasible directions method is used.

Evaluations of this methodology to minimize the matrix residual stress of two typical unidirectional MMC systems: an ultra high modulus graphite (P100)/copper and a silicon-carbide (SiC)/titanium (Ti-15-3) composite, are presented. These MMCs were selected for the availability of data and their acceptance as potential material systems for high temperature applications. Minimization of residual stresses was preferred in the evaluations for its simplicity and to comply with previous related work. However, it is mentioned that the optimum stress state also depends on subsequent thermomechanical loading and this issue will be addressed by the authors in the near-future.

2. COMPOSITE MECHANICS

The composite behavior during fabrication is computationally simulated with nonlinear composite mechanics developed by Chamis and co-workers [7-9] at NASA Lewis Research Center. An in-house program called METCAN (METal matrix Composite ANalyzer) has been developed to simulate the behavior of the MMCs. The mechanics incorporate a multi-cell model packed in a square array, an idealization of a single unit cell as shown in Fig. 1. The mechanics take into account three material phases and assume average stresses in the three microregions (A, B, C) of the constituents (fiber/interphase/matrix), temperature effects, and the nonlinear stress-strain behavior.

The formulation of the composite mechanics was based on the principles of displace-

ment compatibility and force equilibrium. The micromechanics involve closed-form expressions to predict equivalent homogeneous properties for the unidirectional fiber-reinforced ply, more specifically, ply equivalent thermal and mechanical properties, ply inplane uniaxial strengths, and thermomechanical constituent stresses. Further details of the micromechanics equations are summarized in reference [9].

To account for the nonlinear constitutive relationships, the following equation correlates the in-situ constituent properties P to state-variables such as temperature (T) and stress (σ):

$$\frac{P_j^t}{P_{oj}} = [\frac{T_{Mj} - T^t}{T_{Mj} - T_o}]^q [\frac{S_j^t - \sigma_j^t}{S_j^t}]^p \qquad j = m, i, f \tag{1}$$

Properties determined using this equation are the moduli (E), Poisson's ratios (ν), strengths (S), and CTE (α) of the constituents. Subscripts M and o represent the melting and reference conditions, subscript j indicates the matrix (m), interphase (i), or fiber (f). Superscript t represents time at any load step. However, time effects, such as, creep and stress relaxation have been neglected. Each term on the right hand side of eq. 1 represents a monotonic functional dependence of $\frac{P_j^t}{P_{oj}}$ from some reference property value to a terminal or ultimate material state. The specific shape of the function depends on the exponents; thus, exponents (q and p) in eq. 1 are estimated from correlations with experimental data. Here, the first term represents the temperature effects and the second term the inelastic effects of high stresses. Because of the material non-linearity expressed by eq. 1, the calculation of composite properties and microstresses at each time step of the simulated fabrication phase requires an iterative solution of the governing equations.

3. OPTIMIZATION OF INTERPHASE/FABRICATION

The proposed method aims to minimize the residual matrix microstresses by optimizing: (1) mechanical and geometrical characteristics of the interphase; (2) the temperature and consolidation pressure; and (3) the fiber volume ratio. Considering the large number of parameters and the complexity of the simulation, this may be best accomplished with non-linear mathematical programming (NLP). It is recalled that a standard constrained

NLP problem involves the minimization of an objective function:

$$\min \ F(\mathbf{z}) \tag{2.1}$$

subject to constraints of the following form:

$$\mathbf{z}^L \leq \mathbf{z} \leq \mathbf{z}^U \tag{2.2}$$

$$\mathbf{Q}(\mathbf{z}) \leq 0 \tag{2.3}$$

The design variables are represented by the vector z with U and L indicating upper and lower bounds. Also, $\mathbf{Q}(\mathbf{z})$ are the inequality performance constraints. Equations 2.2 and 2.3 define the feasible region for the optimization variables.

In the present paper the objective function is set to minimize matrix stresses in region A. The reduction of matrix residual stresses has been stated as an acceptable objective by many researchers. Although minimum matrix stresses do not neccesserily represent an optimum stress state, this objective is sufficient to demonstrate the method and to obtain comparable results with previous work [5,6]. In the case of open-die consolidation (ie. application of equal pressure in both transverse directions 22 and 33, and no pressure in the longitudinal direction 11), only the normal microstresses σ_{mA11} and σ_{mA22} (where $\sigma_{mA22} = \sigma_{mA33}$) exist in the matrix (region A). Among the many possible ways for these stresses to be minimized simultaneously, the mini-max formulation, that is minimize the maximum stress, is proposed for its tendency to result in equal minimum stresses. Therefore, the optimal fabrication problem is first formulated as the following constrained optimization,

$$\min(\max\{w_1\sigma_{mA11}, w_2\sigma_{mA22}\}) \tag{3}$$

subject to upper and lower bounds (2.2) on the optimization vector z. The optimization vector includes: (1) critical mechanical properties of the candidate interphase layer in reference conditions, such as, the modulus, ultimate strength, and CTE; and (2) the temperatures, consolidation pressures, and times at n_p control points defining, $n_p - 1$ segments of linear temperature and pressure variations. Weighing coefficients (w) in the above objective function are used to indicate the importance of one stress over another.

Constraints are also imposed on the matrix (m), interphase (i), and fiber (f) microstresses at n_s time steps in the form of the maximum stress criterion,

$$S^t_{CmIJ} < \sigma^t_{mIJ} < S^t_{TmIJ} \tag{4.1}$$

$$S^t_{CiIJ} < \sigma^t_{iIJ} < S^t_{TiIJ} \tag{4.2}$$

$$S^t_{CfIJ} < \sigma^t_{fIJ} < S^t_{TfIJ} \tag{4.3}$$

The subscripts C and T identify compressive and tensile strengths respectively, and IJ indicate the applicable stress direction. An additional constraint is imposed on the interphase thickness h_i, to ensure topological compatibility in the case of square packing of fibers:

$$1 + \frac{2h_i}{d_f} - \sqrt{\frac{\pi}{4k_f}} \leq 0 \tag{5}$$

whereas, d_f is the fiber diameter and k_f is the fiber volume ratio.

The presence of residual microstresses affects the in-situ nonlinear properties of the constituents (l) and degrades the properties of the composite. To ensure that the critical properties of the fabricated composite will remain within acceptable limits, lower bounds (L) are imposed on the longitudinal and transverse moduli and strengths of the fabricated composite, these lower bounds are defined by the user.

$$E_{l11} \geq E^L_{l11} \tag{6.1}$$

$$E_{l22} \geq E^L_{l22} \tag{6.2}$$

$$S_{l11} \geq S^L_{l11} \tag{6.3}$$

$$S_{l22} \geq S^L_{l22} \tag{6.4}$$

The optimization criteria described by eqs. 3-6 are transformed to an equivalent NLP compatible formulation (eqs. 1) as follows:

$$\min(\zeta) \tag{7.1}$$

subject to constraints,

$$w_1 \sigma_{mA11} \leq \zeta \tag{7.2}$$

$$w_2 \sigma_{mA22} \leq \zeta \tag{7.3}$$

in addition to constraints (2.2) and (4-6). The objective function ζ is an additional design variable.

The computational procedure for the solution of the optimization problem is schematically shown in Figure 2. Furthermore, the NLP problem described by eqs. 2-7 is numerically solved with the modified feasible directions non-linear programming method [10]. The modified feasible directions algorithm performs a direct search within the feasible optimization domain. The search direction is estimated from first order sensitivity of the objective function and the active constraints. A line search follows along the calculated search direction. The implemented algorithm includes an active set strategy, ie., only the constraints near violation are included in the search, thus allowing the efficient handling of the large number of constraints defined by eqs. 4-6.

4. APPLICATION AND DISCUSSION

This methodology was applied to optimize the interphase characteristics concurrently with the cool-down phase for the following two unidirectional MMCs: (1) ultra-high modulus graphite (P100)/copper, and (2) Silicon carbide (SiC)/titanium (Ti-15-3). Initial data for the fabrication processes for the MMC systems were provided by the Materials Division of NASA Lewis Research Center. These MMCs were selected for the availability of data. Representative constituent properties of the composites at reference conditions ($21°C$, 0 MPa) are shown in Table 1.

4.1 Assumptions

Only the cool-down phase of the fabrication process was simulated during the optimization and thermo-mechanical response since it was assumed that residual stresses are negligable up until this phase. The cool-down phase was subdivided into four increments of linearly varying temperature and pressure. Stress constraints were imposed at five evenly spaced time intervals in each linear segment. In this manner, twenty constraints were introduced for each microstress inequality described in eq. 4, and when the interphase was optimized one additional constraint (eq. 5) on the thickness was added. The lower limits on the composite properties, that is, E^L and S^L, in eq. 6 were assumed to be 90% of the

predicted composite properties of the initial process. The weighing coefficients in eq. 3 were: $w_1 = w_2 = 1$.

Initial interphase properties were assumed equivalent to the matrix properties. In addition to the material properties, the initial interphase thickness was 12% of the fiber diameter and the FVR of the composite system was 40%. When the fabrication process was included in the optimization, the temperatures, pressures, and times at the starting and final points of the four linear segments were used as optimization parameters. The temperature at the beginning of the cool-down phase was held constant and equal to the respective temperature of the initial processes, and the final pressure was set equal to zero. Shown below are the upper and lower bounds imposed on the optimization varibles in accordance with eq. 2.2.

Interphase Properties:

$$34.6GPa \leq E_i \leq 220.8GPa \tag{8.1}$$

$$1.00\mu m/m/^oC \leq \alpha_i \leq 30.0\mu m/m/^oC \tag{8.2}$$

$$34.5MPa \leq S_i \leq 414.0MPa \tag{8.3}$$

Micromechanical Parameters:

$$0.05 \leq \frac{h_i}{d_f} \leq 0.15 \tag{8.4}$$

$$0.05 \leq k_f \leq 0.55 \tag{8.5}$$

Fabrication Process Parameters:

$$T_o \leq T \leq T_M \tag{8.6}$$

$$0 \leq p \leq 345MPa \tag{8.7}$$

$$10sec \leq t \leq 18000sec \tag{8.8}$$

4.2 Case 1: P100/Cu

Shown in Table 2 are the initial (equivalent to the matrix) and resultant optimum interphase properties for two different case studies: (1) the prediction of optimal interphase layer characteristics; and (2) concurrent tailoring of the interphase layer with optimal fabrication considerations, along with the optimum FVR. As seen in Table 2, the interphase thickness always increased to the upper bound in accordance with eq. 8.4. The FVR for both optimization cases slightly decreased in magnitude. Also, the modulus and strength increased for both optimization cases, indicating that a compliant layer may not be suitable to reduce the residual stresses, particularly, in the presence of constraints in eqs 4 and 6. However, a significant difference between the interphase and coupled interphase/fabrication optimization was the different optimum CTE values which decreased in the first case and increased in the latter. This difference seems directly linked to the inclusion of the fabrication process into the optimization, as explained in the next paragraphs.

Figure 3 shows the initial and optimum fabrication processes for the P100/copper MMC. Most notable is the fact that as the predicted optimal temperature drops to reference conditions, the consolidation pressure increases to significantly higher values than the pressure of the initial process. This indicates that significant portions of thermal strains are forced to be developed when the matrix and interphase are highly nonlinear and nearly "plastic", hence high strains result in low stresses. The pressure is removed after the temperature reaches the room value as it does not contribute any further. The maximum value of the consolidation pressure is controlled by the current strength of the constituents, as indicated by the observed active constraints (eq. 4).

The most interesting observation, however, is the development of benificial coupling between optimum consolidation pressure and the optimum CTE for the concurrent interphase/fabrication optimization case which demonstrated significant potential for further reductions in the final matrix microstresses. As depicted in Fig. 4, the interphase optimization only resulted in low stress reductions, as the final maximum matrix microstress, σ_{m11A}, was reduced by only 7%, whereas the transverse microstresses, σ_{m22A}, increased by 13%. However, in the concurrent interphase/fabrication optimization case both residual stresses, σ_{m11A} and σ_{m22A}, were drastically reduced by 49% and 29% respectively. For a thin interphase coating to reduce the matrix stresses, high modulus and high CTE are

required, which in turn will result in very high microstresses in the interphase. As the magnitude of the interphase stresses is controlled by constraints (eq. 4.2), the only obvious combination in connection with the requirement for high composite properties, seems to be an interphase with reduced CTE and higher modulus. This seems to agree also with some conclusions in refs. [5,6], which further reinforces the results and explains why interphase tailoring without fabrication consideration may be ineffective. The concurrent optimization of the fabrication process with the interphase characteristics remedied the problem of high stresses in the interphase, as a result of the high consolidation pressure effects discussed in the previous paragraphs. Any reductions in the interphase stresses, attained via fabrication parameters, allowed much higher values in the interphase CTE and modulus which further reduced the matrix stresses. In this manner a benificial coupling between process and interphase was established. The significance of the coupling mechanism is demonstrated by the drastic reductions in the matrix stresses.

An important aspect in the reduction of the residual stresses is the avoidance of degradation in the predicted final properties of the composite. The introduction of the composite constraints represented by eq. 6 proved to be a vital addition to the methodology. The added constraints on the composite properties ensured a high-performance final composite material with minimal property degradation, as shown in Table 3. In addition, the combined interphase/fabrication optimization produced improved composite properties when compared to individual interphase optimization only, except for the transverse modulus. The slight reduction in the composite properties when compared to the initial case can be attributed to the decrease in FVR. From previous observed results by the authors, the addition of the composite property constraints directly led to a better definition of the problem. This can be attributed to a more confined and convex feasible design space which led to the exclusion of many local minima. As a result, a faster convergence was achieved within the feasible domain.

4.3 Case 2: SiC/Ti-15-3

The optimization of the SiC/Ti-15-3 MMC also illustrated the importance of coupling the interphase and fabrication process. Referring to Table 4, the optimum interphase modulus and strength increased drastically compared to the initial and interphase/fabrication

optimization cases, though the modulus and strength did increase slightly for the interphase/fabrication optimization case, again not supporting the theory of a compliant interphase. In both optimization cases the CTE increased to nearly equivalent values. Interphase thickness, as in the previous case, reached the upper bound. Finally, the FVR decreased slightly for both optimization case studies. The predicted interphase modulus and strength when the interphase was optimized alone, was unrealistically high compared to the more realistic modulus and strength of the concurrent interphase/fabrication optimization and the nearly equivalent CTEs, which clearly demonstrates the merits of the concurrent interphase/fabrication tailoring and indicates the importance of the coupling effect in reducing the matrix microstresses.

The optimum fabrication process for the interphase/fabrication optimization is depicted in Fig. 5. The consolidation pressure reached significantly higher pressures than the initial process, following a similar trend with the P100/copper case. To achieve these results, initial starting points had to be changed to avoid local minima during the optimization search. Fig. 6 depicts the microstress build-up for the initial and optimized cases. The longitudinal microstress σ_{m11A} was reduced by 65% and 98% in the interphase optimization alone and concurrent interphase/fabrication optimization, respectively. Whereas, the transverse microstress, originally the maximum stress, was reduced by 77% for the interphase optimization alone and 99% for the coupled interphase/fabrication optimization. The magnitude of the reduction in microstresses demonstrates the importance of tailoring concurrently the interphase with fabrication considerations.

The predicted final composite properties, depicted in Table 5, did not degrade and in most instances improved compared to the initial process. The greatest improvement was achieved in the transverse composite properties for both optimization cases. Strength and stiffness increased for the optimized fabricated composite due to the addition of the interphase layer.

5. SUMMARY

A method was presented for tailoring the interphase layer characteristics for unidirectional metal-matrix composites for minimal residual stresses with concurrent fabrication

considerations. The thermomechanical response of the fabricated MMC and the development of residual stresses was simulated based on nonlinear micromechanics. The NLP problem was numerically solved with the modified feasible directions nonlinear programming method. Other performance criteria included stress failure constraints, and lower bounds on critical properties of the fabricated composite. The optimized interphase characteristics included the modulus, strength, CTE, thickness and FVR. The fabrication parameters involved the temperature and pressure histories. An in-house research code has been developed incorporating this method.

Applications were performed on ultra-high modulus graphite (P100)/copper and SiC/Ti-15 composites. Obtained results from the concurrent interphase and fabrication optimization were compared with results from interphase tailoring without fabrication considerations and a currently used fabrication process. For the case of P100/Copper, the results indicated that interphase tailoring alone may not be a viable way to reduce matrix stresses without failures in the interphase and/or reduced composite properties. Contrary, the interphase tailoring with simultaneous fabrication consideration was proved effective in reducing residual stresses, in that, proper combinations of processing temperature and high consolidation pressure removed the problem of high stresses in the interphase. The results for the SiC/Ti-15-3 MMC indicated that interphase tailoring alone can be effective in reducing the residual stresses, however, the interphase optimization under elevated consolidation pressure produced significant additional reductions. Hence, a strong coupling mechanism was revealed between interphase and fabrication tailoring, which resulted in significant residual stress reductions. The incorporation of unified non-linear composite mechanics enabled the capture of the coupling. Overall, the results illustrated the significance of concurrent interphase with fabrication tailoring, and demonstrated the capabilities and effectiveness of the developed methodology.

6. REFERENCES

1. R. A. Naik, W. S. Johnson, and W. D. Pollock, "Effect of a High Temperature Cycle on the Mechanical Properties of Silicon Carbide/Titanium Metal Matrix Composites," *Symposium on High Temperature Composites*, June, 1989.

2. T. P. Gabb, J. Gayda, and R. A. MacKay, "Isothermal and Nonisothermal Fatigue Behavior of a Metal Matrix Composite," *Journal of Composite Materials*, in press
3. M. G. Castelli, J. R. Ellis, and P. A. Bartolotta, "Thermomechanical Testing Techniques for High-Temperature Composites: TMF Behavior of SiC(SCS-6)/Ti-15-3," *NASA TM-103171*, 1990.
4. D. A. Saravanos, P. L. N. Murthy, and M. Morel, "Optimum Fabrication Process for Unidirectional Metal Matrix Composite: A Computational Simulation," *35th International SAMPE Symposium/Exhibition*, 1990; (also *NASA TM 102559*, 1990).
5. L. J. Ghosn and B. A. Lerch, "Optimum Inteface Properties for Metal Matrix Composites," *NASA TM 102295*, 1989.
6. S. Jansson and F. A. Leckie, "Reduction of Thermal Stresses in Continuous Fiber Reinforced Metal Matrix Composites With Interface Layers," *NASA CR 185302*, 1990.
7. C. C. Chamis, P. L. N. Murthy and D. A. Hopkins, "Computational Simulation of High Temperature Metal Matrix Composites Cyclic Behavior", *NASA TM 102115*, 1988.
8. P. L. N. Murthy, D. A. Hopkins and C. C. Chamis, "Metal Matrix Composite Micromechanics: In-Situ Behavior Influence on Composite Properties," *NASA TM 102302*, 1989.
9. D. A. Hopkins and C. C. Chamis, "A Unique Set of Micromechanics Equations for High Temperature Metal Matrix Composites", *NASA TM 87154*, 1985.
10. G. N. Vanderplaats, *Numerical Optimization Techniques for Engineering Design: With Applications*, McGraw-Hill Book Company, New York, 1984.

Table 1. Representative constituent mechanical properties of composite systems at reference conditions.

P100 Graphite	Copper
$E_{f11} = 724.5\ GPa$	$E_m = 122.1\ GPa$
$E_{f22} = 6.21\ GPa$	
$G_{f12} = 7.59\ GPa$	$G_m = 47.0\ GPa$
$G_{f23} = 4.83\ GPa$	
$\rho_f = 2.16\ g/cm^3$	$\rho_m = 8.86\ g/cm^3$
$\nu_{f12} = 0.20$	$\nu_m = 0.30$
$\nu_{f23} = 0.25$	
$\alpha_{f11} = -1.61\ \mu m/m/°C$	$\alpha_m = 17.5\ \mu m/m/°C$
$\alpha_{f22} = 10.0\ \mu m/m/°C$	
$S_{f11,T} = 2242.0\ MPa$	$S_{mn} = 221.0\ MPa$
$S_{f11,C} = 1380.0\ MPa$	
$S_{f22} = 173.0\ MPa$	
$S_{f12} = 173.0\ MPa$	$S_{ms} = 131.0\ MPa$
$S_{f23} = 86.0\ MPa$	

SiC	Ti-15-3
$E_f = 427.8\ GPa$	$E_m = 84.9\ GPa$
$G_f = 164.2\ GPa$	$G_m = 32.1\ GPa$
$\rho_f = 3.05\ g/cm^3$	$\rho_m = 4.76\ g/cm^3$
$\nu_f = 0.30$	$\nu_m = 0.32$
$\alpha_f = 4.86\ \mu m/m/°C$	$\alpha_m = 8.04\ \mu m/m/°C$
$S_{fn,T} = 3450.0\ MPa$	$S_{mn} = 897.0\ MPa$
$S_{fn,C} = 4485.0\ MPa$	
$S_{fs} = 2070.0\ MPa$	$S_{ms} = 621.0\ MPa$

Table 2. Initial and Optimized Interphase Properties for P100/Copper at the Beginning of Fabrication

	Initial Interphase	Optimum Interphase	Optimum Interphase/Fabrication
E_i (GPa)	122.1	174.3	166.8
α_i ($\mu m/m/°C$)	17.50	11.20	22.0
S_i (MPa)	221.0	252.0	282.0
h_i/d_f (%)	12	15	15
k_f (%)	40	38	36

Table 3. Select Initial and Optimum Composite Properties for P100/Copper at the End of Fabrication

	Initial Process	Interphase Optimization	Interphase/Fabrication Optimization
E_{l11} (GPa)	284.1	270.0	277.0
E_{l22} (GPa)	16.30	30.0	21.6
α_{l11} ($\mu m/m/°C$)	-1.25	-8.89	0.0670
α_{l22} ($\mu m/m/°C$)	18.8	15.6	20.20
S^T_{l11} (MPa)	905.0	871.0	882.0
S^C_{l11} (MPa)	173.0	169.0	173.0
S^T_{l22} (MPa)	18.0	15.0	18.0
S^C_{l22} (MPa)	38.0	32.0	36.0

Table 4. Initial and Optimized Interphase Properties for SiC/Ti15-3 at the Beginning of Fabrication

	Initial Interphase	Optimum Interphase	Optimum Interphase/Fabrication
E_i (GPa)	84.9	182.2	92.9
α_i $(\mu m/m/^\circ C)$	8.04	13.6	13.7
S_i (MPa)	897.0	1060.0	906.0
h_i/d_f (%)	12	15	15
k_f (%)	40	35	37

Table 5. Select Initial and Optimum Composite Properties for SiC/Ti15-3 at the End of Fabrication

	Initial Process	Interphase Optimization	Interphase/Fabrication Optimization
E_{l11} (GPa)	214.2	210.0	206.8
E_{l22} (GPa)	128.3	146.8	128.3
α_{l11} $(\mu m/m/^\circ C)$	6.02	7.25	6.90
α_{l22} $(\mu m/m/^\circ C)$	6.83	8.46	8.28
S^T_{l11} (MPa)	1740.0	1730.0	1689.0
S^C_{l11} (MPa)	436.0	970.0	955.0
S^T_{l22} (MPa)	47.0	119.0	103.6
S^C_{l22} (MPa)	714.0	1647.0	1424.9

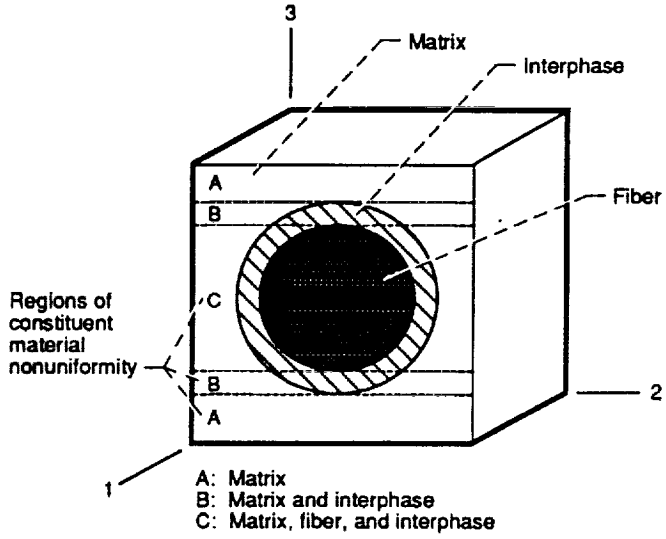

Figure 1.—Material microregions in a representative MMC cell.

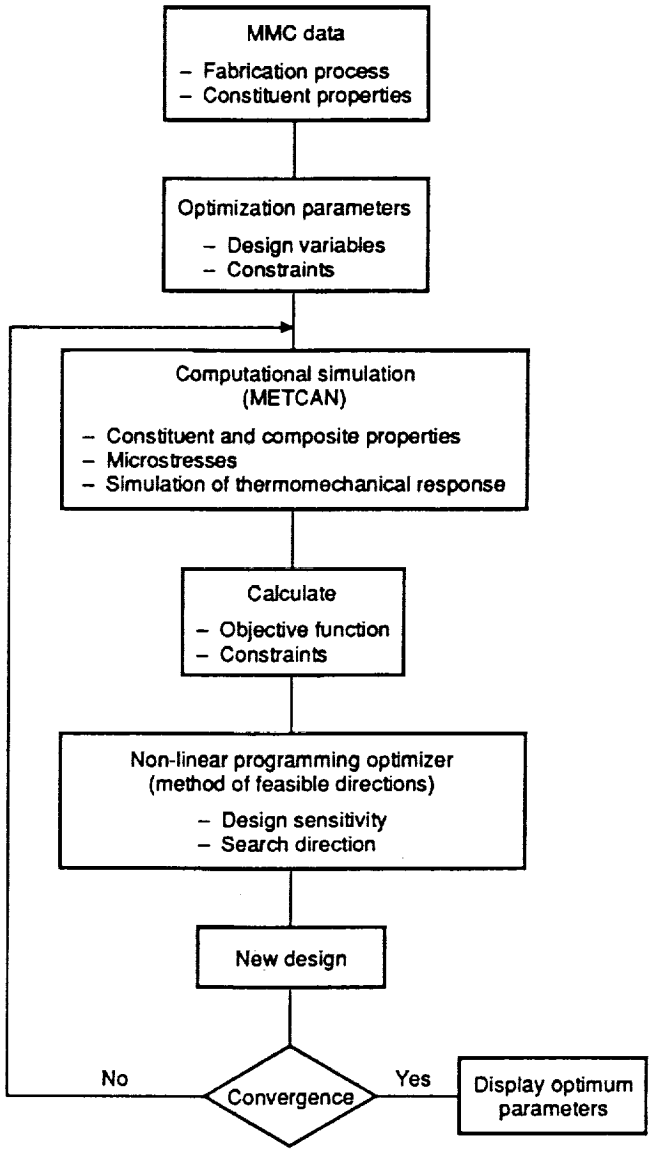

Figure 2.—Computational procedure to concurrently optimize the fabrication process and interphase.

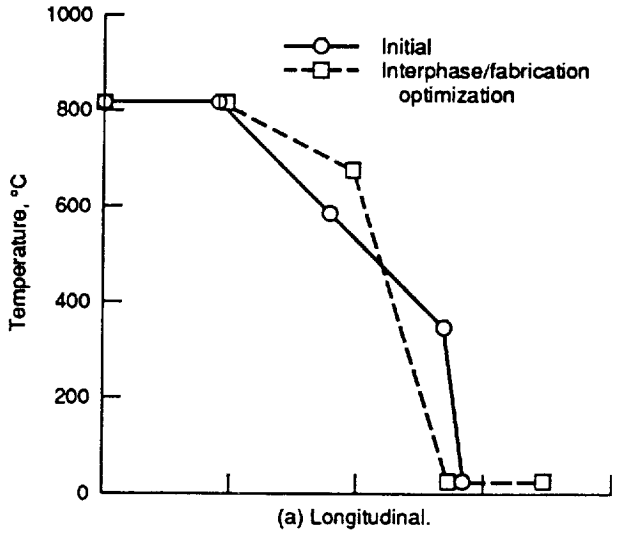

(a) Longitudinal.

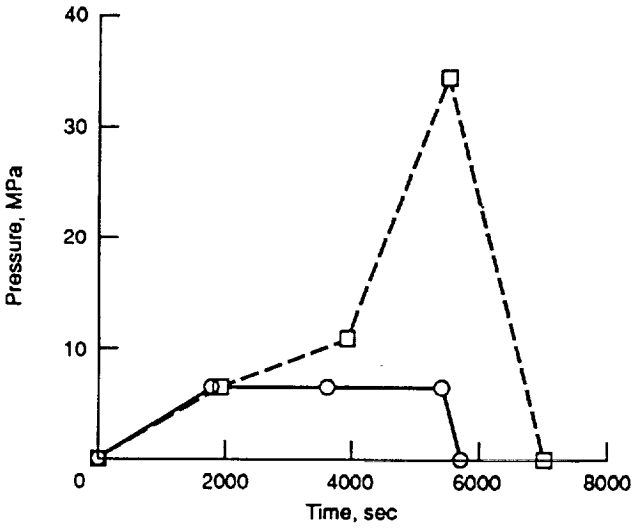

(b) Transverse.

Figure 3.—Optimum and initial cool-down phases for P100/copper.

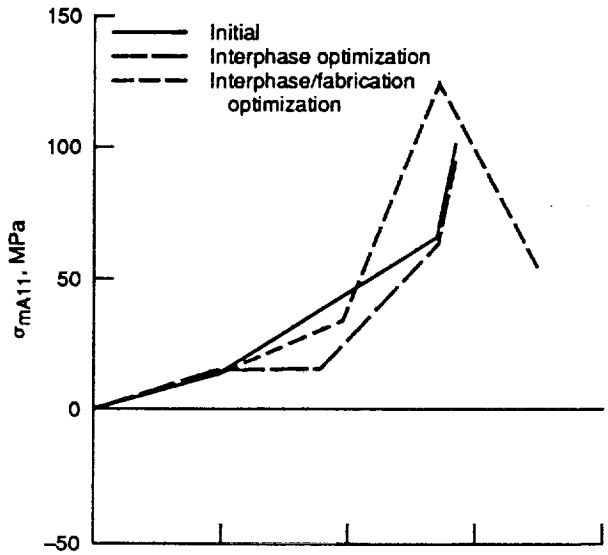

(a) Longitudinal.

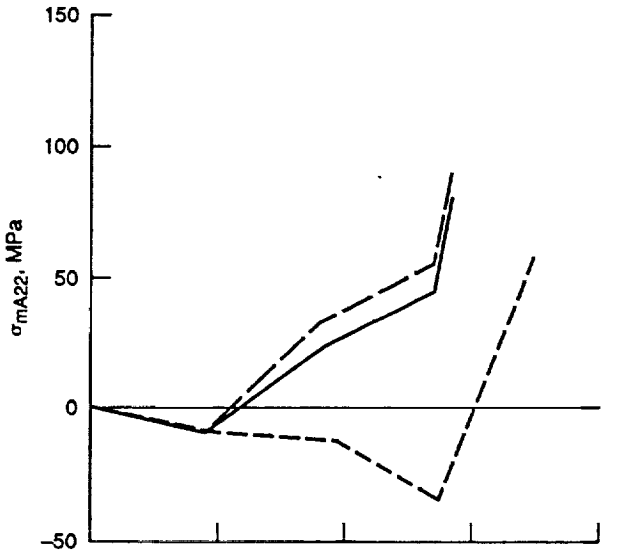

(b) Transverse.

Figure 4.—Matrix microstresses developed during the cool-down phase of P100/copper.

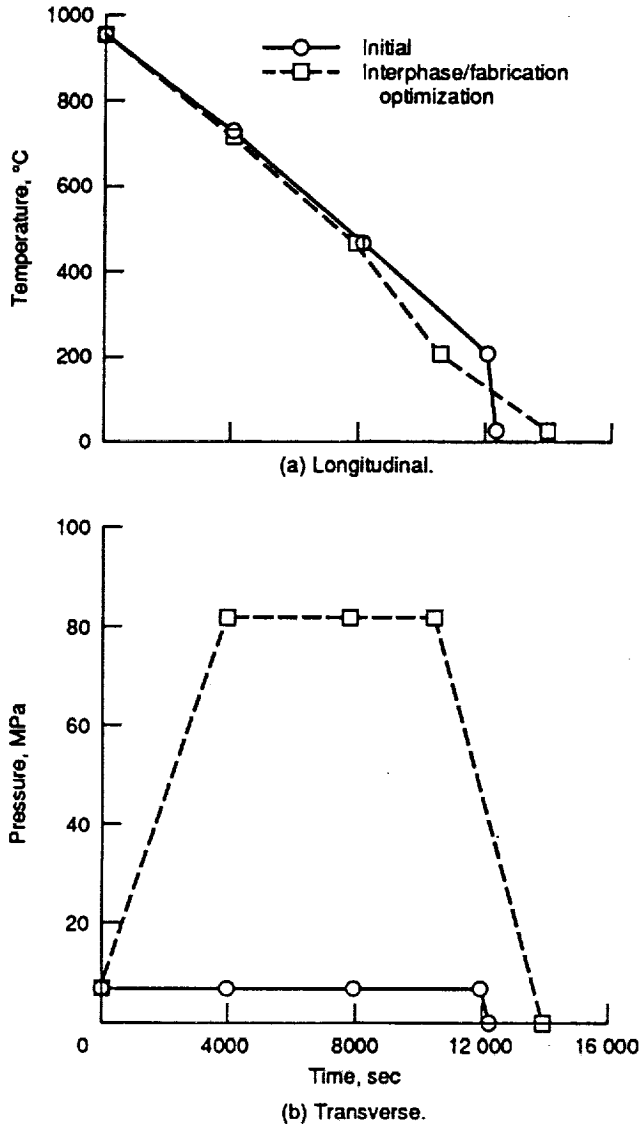

(a) Longitudinal.

(b) Transverse.

Figure 5.—Optimum and initial cool-down phases for SiC/Ti15-3-3-3.

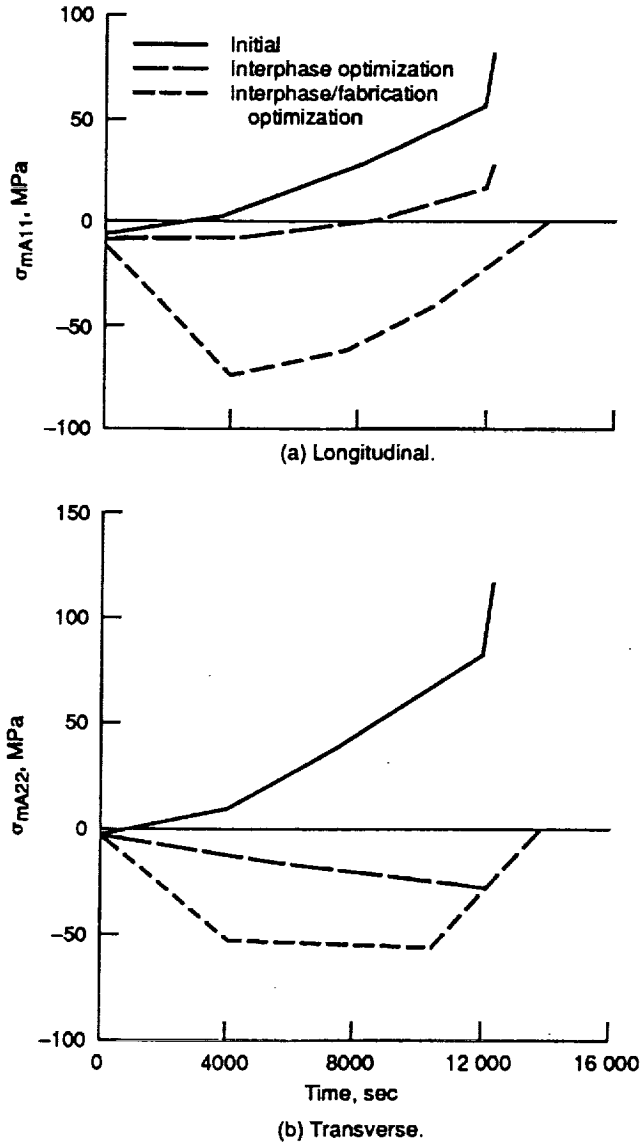

(a) Longitudinal.

(b) Transverse.

Figure 6.—Matrix microstresses developed during the cool-down phase of SiC/Ti15-3-3-3.

REPORT DOCUMENTATION PAGE

Form Approved
OMB No. 0704-0188

1. AGENCY USE ONLY (*Leave blank*)	2. REPORT DATE	3. REPORT TYPE AND DATES COVERED
		Technical Memorandum

4. TITLE AND SUBTITLE
Interphase Layer Optimization for Metal Matrix Composites With Fabrication Considerations

5. FUNDING NUMBERS
WU-510-10-50

6. AUTHOR(S)
M. Morel, D.A. Saravanos, and C.C. Chamis

7. PERFORMING ORGANIZATION NAME(S) AND ADDRESS(ES)
National Aeronautics and Space Administration
Lewis Research Center
Cleveland, Ohio 44135-3191

8. PERFORMING ORGANIZATION REPORT NUMBER
E-6457

9. SPONSORING/MONITORING AGENCY NAMES(S) AND ADDRESS(ES)
National Aeronautics and Space Administration
Washington, D.C. 20546-0001

10. SPONSORING/MONITORING AGENCY REPORT NUMBER
NASA TM-105166

11. SUPPLEMENTARY NOTES Prepared for the 36th International SAMPE Symposium and Exhibition, San Diego, California, April 15-18, 1991. M. Morel, Sverdrup Technology, Inc., 2001 Aerospace Parkway, Brook Park, Ohio 44142; D.A. Saravanos, Case Western Reserve University, Cleveland, Ohio 44106; C.C. Chamis, NASA Lewis Research Center. Responsible person, M. Morel, (216) 826-2284.

12a. DISTRIBUTION/AVAILABILITY STATEMENT
Unclassified - Unlimited
Subject Category 24

12b. DISTRIBUTION CODE

13. ABSTRACT ***(Maximum 200 words)***

A methodology is presented to reduce the final matrix microstresses for metal matrix composites by concurrently optimizing the interphase characteristics and fabrication process. Application cases include interphase tailoring with and without fabrication considerations for two material systems, graphite/copper and silicon carbide/titanium. Results indicate that concurrent interphase/fabrication optimization produces significant reductions in the matrix residual stresses and strong coupling between interphase and fabrication tailoring. The interphase coefficient of thermal expansion and the fabrication consolidation pressure are the most important design parameters and must be concurrently optimized to further reduce the microstresses to more desireable magnitudes.

14. SUBJECT TERMS
Composites; Metal matrix; Optimization; Interphase; Fabrication process; Residual stresses

15. NUMBER OF PAGES
22

16. PRICE CODE
A03

17. SECURITY CLASSIFICATION OF REPORT	18. SECURITY CLASSIFICATION OF THIS PAGE	19. SECURITY CLASSIFICATION OF ABSTRACT	20. LIMITATION OF ABSTRACT
Unclassified	Unclassified		